Categorization of Alzheimer's Disease using Orthogonal Moments in Hough and Radon Space

Ramesh Munirathinam[1], Bhuvaneswari Balachander[2]

[1]Department of Biomedical Engineering, Karpagam Academy of Higher Education, Coimbatore, Tamilnadu, India

[2]Department of Electronics and Communication Engineering, Saveetha School of Engineering, Saveetha Institute of Medical and Technical Sciences Chennai, Tamilnadu, India

rameshmunirathinam@gmail.com

Abstract: Alzheimer's disease is found to have the preclinical phase which involves the changes in behaviroal and psycholog- ical functions of an individual. It is found that the alteration of cerebellar region influences the behaviroal abilities of an in- dividual. In this work, the MRI data is obtained from OASIS database. The subjects were grouped into three classes namely normal (CDR=0), Mild Cognitive Impaired (MCI)(CDR=0.5) and Alzheimer Demented Subjects (AD)(CDR=1,2) based on the CDR scores provided in the database. The cerebellar re- gion is delineated from the MRI images using level set method and the orthogonal Zernike moments are extracted from seg- mented image and also from Hlough and Radon spaces of the segmented cerebellum. Results show that the level set method delineated the cerebellum by preserving the edge points. Higher order moments extrated from the segmented cerebellum show better discriminating ability between normal, MCI and AD sub- jects. Hough and Radon transforms have the ability to capture the defined edge points and continuous boundary of the cerebel- lar region which helps in retaining the structure of the cerebel- lum. The features extracted from the Hough and Radon spaces show that the definable lower order moments show promising discrimination of AD subjects from normal and MCI subjects.

Keywords: Alzheimer's Disease, Cerebellum, Hough Transform, Radon Transform, Shape analysis, Zernike Moments

DOI Number: 10.48047/nq.2022.20.19.NQ99193 **NeuroQuantology2022;20(19): 2291-2300**

I.Introduction

Alzheimer's Disease (AD) is a common brain disorder preva- lent in the elderly [1]. Previous researches on Alzheimer's included on the changes in hypothalamus but the changes in the cerebellum were not focussed much, the cerebellum which is responsible for the motor functions [2]. The progression of Alzheimer's will vary over time, although the time may vary for every patient. In general the development of the disease includes three stages namely early stage, mild stage and late stage. Symptoms of the disease include decline in memory, depressed mood, declined language, disorientation, behaviour deficits [3]. Clinical diagnosis of Alzheimer's include medical examination, neuroimag- ing, analysis of cerebrospinal fluid, examination of blood samples. Structural and functional MRI and PET are also considered as screening tools in disease diagnosis for cere- bral metabolism and amyloid assessment [4]. Progressive cerebral atrophy that determines neurodegeneration can be visualised using MRI [5]. It has also been observed that from

MRI brain regions such as hippocampus, parahippocampus, temporal lobe, frontal lobe and precuneus show structural atrophy for patients with Alzheimer's [6].

Cerebral surface area in the brain was significantly smaller, significant reduction in cortical thickness and surface area atrophy in a wide region of the prefrontal lobe, temporal and lateral occipital cortex of the brain were also found in patients during Alzheimer's [7]. The posterior lobe of the cerebellum is affected during the early stages followed with the anterior lobes when the disease progresses. Cerebellar white matter reduces in volume than grey matter [8]. P-type Fourier descriptors were used to evaluate the shape defor- mation of the brain to analyse the morphological changes which helped in early identification of the diseases with an accuracy of 87% [9]. Spherical harmonics approaches were used to classify the hippocampus shape features in order to discriminate between Alzheimer's and Mild Cognitive Im- pairment (MCI) [10]. Radon transform which is a spherical case of Trace Triplet transform were used to detect textural variations in the brain [11]. Hough Transform is used to determine the region of interest around the organs to estimate the texture feature variations [12]. Radon transformation of multi-overlapping windows is presented to efficiently detect the optic nerve head in both color and fluorescein angiography retinal fundus images. Radon transformation has better detection rates for different structural, colour and intensity variations [13].

II.Literature Review

Alzheimer's is a progressive neurological disorder that causes shrinking of the brain, thereby making the brain cells die that leads to memory loss. It is estimated that around 6% of the population aged above 65 are affected by the disease [14]. People affected by Alzheimer's will experience symptoms including memory loss, cognitive deficits, recognition problems, difficulties in reading, writing and speaking, personality changes. The disease progression includes mild or early stages with an average time frame of 2 to 4 years, moderate or middle stage with a time frame of 2 to 10 years and severe or late stage with an average time frame of 1 to 3 years. Some of the major reasons for late diagnosis is that the early stage signs are usually not recognized or mistaken as signs of aging. Timely diagnosis offers better early intervention steps thereby improving patient safety, reduction in the cost involved, etc. [20].

The first diagnostic test in patients for cognitive impairment is through brain MRI [16]. Alzheimer's disease is a type of dementia that is pathologically characterized by the presence of β-amyloid plaques and neurofibrillary tangles [17]. Upto 65% of patients diagnosed with Alzheimers have genetic mutation in the amyloid precursor protein (Alzheimer's Association, 2015). Apart from the most common symptoms of the disease which could vary based on the age and the individuals. Alzheimer's disease causes malfunction of neurons from various parts of the brain which inturn affects the daily activities, mood swifts, personality disorders, difficulty in problem solving but the degree of decline varies between person to person [18]. Few other symptoms noticed in patients include bowel and bladder problems, infection, broken bones resulting due to the imbalance (Higuera, 2017).

The diagnostic procedures include neuropsychological tests and serologic tests for biomarkers, other routine tests including blood cell count test, thyroid hormone stimulation test, folate and vitamin B-12 tests

are utilized by medical practitioners along with MRI. Diagnosis is based on the biomarker identification which includes hippocampal atrophy on MRI scans, cerebrospinal fluid markers, positive amyloid imaging and skin biopsy (Qing Meng et al, 2020). Cognitive impairment can be identified through mental assessment, neuropsychological testing and monitoring the disease progression [19]. Nowadays biomarkers are also incorporated in dementia diagnosis to identify accumulation of amyloid-ß protein, neuronal injury and degeneration and also synaptic dysfunction [20].

Pathophysiological changes in the brain include alterations in Cerebrospinal Fluid (CSF) based Aß-42 and also increase in Amyloid leading to cognitive impairment, these changes can be visualised through PET based resting glucose metabolism and MRI [21]. A combination of brain volumet- rics and PET showed that hypometabolism had exceeded grey matter atrophy in people with Alzheimer's [22].

Shabana Urooj et al (2021) [23] proposed a hybrid method for detecting Alzheimer's at early stages using Polar Har- monic Transforms (PHT) and Self-adaptive Differential

Evolution Wavelet Neural Network (SaDE-WNN) using orthogonal moments through which features are extracted from grey matter tissue from MRI. The proposed method overcomes the drawbacks of wavelet neural networks such as initial tuning and parameter setting. The speed of compu- tation in PHT is faster when compared to Zernike moments, numerically stable, robust to noise and better performance in image analysis.

K. P. Philip et al (1994) [12]presented an algorithm using approximate geometric models of regions of interest in organs to identify the estimated location of the organ such as chest walls in humans and left ventricular contours of dog heart using Fuzzy Hough transform (FHT). FHT helps in detecting organs whose shapes for image analysis over conventional pattern recognition techniques which are not capable of identifying the shape of the organs. The identified contours contain discontinuities as the algorithm operates independently at each point of the model. Fayyaz Ahmad et al (2018) [24] proposed an approach that classified different stages in Alzheimer's Disease using Principal Component Analysis (PCA) on face images. Activated voxels of the hippocampus were given as vectors of covariance matrices using which eigenvectors were obtained which helped in the classification of disease as the hippocampus of the brain gets affected in the beginning stages of Alzheimers.

Ning Wang et al (2020) [25] showed a t-distributed stochas- tic neighbor embedding machine learning algorithm based supervised clustering of anomaly detection with linguistic biomarkers which is suitable for visualising high dimen- sional datasets for early detection of Alzheimer's. Achraf Ben Miled et al (2020) [26] proposed a classification archi- tecture to implement a pre-trained network AlexNet which detected features from MRI images at the Mild Cognitive Impairment stage (MCI) which obtained a classification accuracy of 96.83%. F. Previtali et al (2016) [27] presented an automated approach that classifies Alzheimer's disease from patient MRI images. Features for classification were extracted using a computer vision method called Oriented FAST and Rotated BRIEF with a classification accuracy of 97%.

U. Rajendra Acharya et al (2019) [28] developed a Com- puter Aided Brain Diagnosis system to identify Alzheimer's. The process consisted of filtering, feature extraction using Shearlet transform and k-Nearest Neighbor

(KNN) based classification. The proposed algorithm provided an accuracy of 94.54%. Yudong Zhanga et al (2016) [29] proposed a novel three dimensional eigenbrain based on eigenface for single photon emission computed tomography (SPECT) im- ages which was an extension of two-dimensional eigenbrain and classified using SVM with a classification accuracy of 92.37%.

Debesh Jha et al (2017) [30] proposed a dual-tree complex wavelet transform (DTCWT) for extracting features from MRI images, Principal component analysis (PCA) is used for reducing the dimensionality of the feature vector. Feed Forward Neural Network (FNN) is used to classify between

Alzheimer's brain data and healthy brain data. The method proposed produced an accuracy rate of 90.06 ± 0.01%. Xi- aolu Zhu et al [31] [32] presented an edge detection method using sobel or canny edge detector and Hough transform for identifying circles for automatically locating the optic disc in the fundus image of retina. Abdullah et al (2016) [33] presented a robust methodology for early detection of eye diseases. In this method the optic disc center is determined using circular Hough transform and the optic disc boundary is segmented using the grow cut algorithm.

III. Materials and Methods

A. Workflow

Workflow involved in this study is represented in Fig.1 can be briefed as follows. At first MRI scans dataset is chosen for this analysis. Pre-processing step is made for converting the images in the dataset into required format. Later, sample size selection is produced using G power software. Segmented the required cerebellum region from the MRI scans. Then moment feature extraction is made by using Zernike mo- ments, radon transformed Zernike moments [34] and Hough transformed Zernike moments. From the extracted 64 mo- ment features, 10 best features are preferred for the classifi- cation.

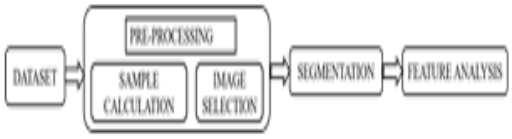

Figure. 1: Process flow of the proposed analysis

B. Dataset

The images used in this analysis are acquired from Open Ac- cess Series of Imaging Studies (OASIS). OASIS is an open access MR image repository for analyzing the morphometric changes that are occuring in the brain due to the incidence of Alzheimer' disease. The subjects were grouped based on CDR score as normal (CDR=0), Mild Cognitive Impar- ied (MCI) (CDR=0.5) and Alzheimer diseased (CDR=1&2). A total of 150 subjects were analyzed with 50 subjects from each group [35].

C.Preprocessing

The MRI data considered for the analysis is found to be in

.hdr format. ImageJ software is used to extract the slice in- formation and the output file is saved in .jpg format.

1) G-Power

The number of samples required for the analysis is obtained using Gpower simulation software. The effect size (d) indi- cating the precise level of identification is assigned as 0.3. The minimum algorithm power (α) is expected to be 80% (0.8). Finally the number of normal (N1) and abnormal (N2) subjects are fixed to be equal for the proposed analy- sis. Based on the prefixed parameters the total number of samples considered for the analysis is 176 [36][37].

2) Image Selection

Each subject has 180 slice information, the volume of the specific brain region can be

analyzed alternatively using the shape measures. The mid slice is found to have the max- imum information about the shape and size of a particular region of interest. In this analysis mid MRI slice information is considered for the analysis.

D.ROI Extraction & Feature Selection

Level set without reinitialization is employed to extract the required cerebellum from the MRI slices. Zernike moments are extracted from the segmented cerebellum, Random trans- formed cerebellum images and Hough transformed cerebel- lum images. The expression of Zernike moments, Radon transform and Hough Transform are not discussed since there is no modification of mathematical expression is done in this work.

IV.Results

Figure 2 represents a normal MR image from the sagittal plane, which shows the cerebrum, grey matter, white matter, corpus callosum, ventricles, thalamus and cerebellum. MR image of the brain with mild cognitive impairment which in- dicates that there is a reduction in the grey matter and white matter level when compared with the normal MR image. There is also a change in the size and shape of the corpus callosum in the MR image representing mild cognitive im- pairment in comparison with the normal MR image. There is also a transition in size of the cerebral ventricles. There are textural variations in grey matter in subjects affected by Alzheimer's disease and also decrease in grey matter volume. Additional grey matter loss is visualised in the thalamus re- gion which leads to cognitive dysfunction. Brain tissue vari- ations are found in the cerebellum of the MR image of MCI and MR image of AD. The hippocampus region of the brain also has some volumetric changes in MCI MR image and the hippocampus suffers more volumetric loss in patients af- fected with AD than patients affected with MCI.

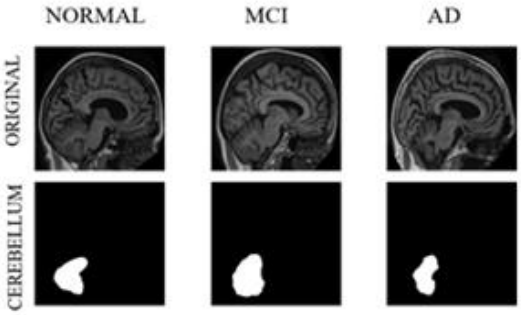

Figure. 2: Illustration of segmented Cerebellum from MR images of Normal, MCI and AD subjects Analysis on the shape changes in the cerebellum is carried by extracting the moment features from segmented cerebellum

Table 1: List of most significant ($p<0.05$) Zernike moment features differentiating normal and MCI subjects using seg- mented cerebellum images

S.No	Feature	Normal Subject	MCI Subject
1	$M_{4,0}$	0.11 ± 0.04	0.67 ± 0.14
2	$M_{6,2}$	0.07 ± 0.03	0.85 ± 0.32
3	$M_{5,1}$	0.08 ± 0.06	0.58 ± 0.21
4	$M_{17,9}$	0.04 ± 0.18	0.66 ± 0.22
5	$M_{11,7}$	0.09 ± 0.04	0.34 ± 0.12
6	$M_{10,8}$	0.07 ± 0.07	0.39 ± 0.14
7	$M_{16,8}$	0.04 ± 0.11	0.42 ± 0.16
8	$M_{10,2}$	0.02 ± 0.12	0.53 ± 0.24
9	$M_{10,2}$	0.02 ± 0.12	0.53 ± 0.24
10	$M_{12,8}$	0.08 ± 0.05	0.37 ± 0.15

Table 2: List of most significant ($p<0.05$) Zernike moment features differentiating normal and AD subjects using seg- mented cerebellum images

S.No	Feature	Normal Subject	AD Subject
1	$M_{14,10}$	0.05 ± 0.04	0.62 ± 0.26
2	$M_{10,6}$	0.06 ± 0.09	0.56 ± 0.21
3	$M_{10,4}$	0.07 ± 0.05	0.48 ± 0.21
4	$M_{9,7}$	0.09 ± 0.06	0.35 ± 0.12
5	$M_{9,3}$	0.05 ± 0.05	0.54 ± 0.26
6	$M_{11,7}$	0.08 ± 0.06	0.36 ± 0.12
7	$M_{12,0}$	0.05 ± 0.07	0.38 ± 0.17
8	$M_{12,8}$	0.07 ± 0.06	0.41 ± 0.17
9	$M_{9,9}$	0.08 ± 0.04	0.68 ± 0.34
10	$M_{5,5}$	0.09 ± 0.05	0.26 ± 0.17

of normal, MCI and AD subjects. The segmented cerebel- lum of the normal brain MR image when compared with MCI MR image seems to have an intermediate volumetric change leading to shape alteration. The segmented result of the cerebellum of patients affected with AD shows vari- ations in the texture of the cerebellum and also a

reduction in volume to a greater extent than mild cognitive impairment.

The analysis was performed by comparing the features of normal, MCI and AD subjects. The MCI subjects were found to have ability of normal subjects thus making it dif- ficult to differentiate between them, therefore first analysis was done by comparing the features of normal and MCI subjects. A total of 64 moments were extracted from the segmented cerebellum and most significant moment features are considered for the analysis. Table 1 describes about the significant features capable of differentiating normal and MCI subjects using Zernike moments. It can be observed that the lower order moment has the high significance in

Table 3: List of most significant ($p<0.05$) Zernike moment features differentiating MCI and AD subjects using segmented cerebellum images

S.No	Feature	MCI Subject	AD Subject
1	$M_{4,0}$	0.68 ± 0.12	0.17 ± 0.10
2	$M_{17,9}$	0.42 ± 0.24	0.33 ± 0.15
3	$M_{6,0}$	1.20 ± 0.65	0.22 ± 0.16
4	$M_{5,2}$	0.9 ± 0.32	0.36 ± 0.17
5	$M_{9,9}$	0.25 ± 0.16	0.68 ± 0.34
6	$M_{11,11}$	0.23 ± 0.18	1.05 ± 0.76
7	$M_{8,8}$	0.17 ± 0.13	0.26 ± 0.17
8	$M_{16,8}$	0.46 ± 0.13	0.29 ± 0.12
9	$M_{13,13}$	0.23 ± 0.16	0.74 ± 0.51
10	$M_{5,1}$	0.62 ± 0.20	0.36 ± 0.18

Table 4: List of most significant ($p<0.05$) Zernike moment features differentiating normal and MCI subjects using Radon transformed cerebellum images

S.No	Feature	Normal Subject	MCI Subject
1	$M_{13,9}$	0.53 ± 0.19	0.28 ± 0.18
2	$M_{8,8}$	0.56 ± 0.22	0.50 ± 0.21
3	$M_{4,2}$	0.56 ± 0.18	0.42 ± 0.21
4	$M_{9,7}$	0.63 ± 0.19	0.43 ± 0.22
5	$M_{13,13}$	0.38 ± 0.22	0.61 ± 0.24
6	$M_{10,10}$	0.54 ± 0.22	0.33 ± 0.22
7	$M_{10,10}$	0.54 ± 0.22	0.33 ± 0.22
8	$M_{8,6}$	0.54 ± 0.19	0.36 ± 0.21
9	$M_{10,6}$	0.58 ± 0.18	0.43 ± 0.19
10	$M_{11,8}$	0.59 ± 0.20	0.41 ± 0.21

Table 5: List of most significant ($p<0.05$) Zernike moment features differentiating normal and AD subjects using Radon transformed cerebellum images

S.No	Feature	Normal Subject	AD Subject
1	$M_{4,2}$	0.59 ± 0.21	0.38 ± 0.25
	$M_{17,9}$	0.60 ± 0.20	0.41 ± 0.30
3	$M_{12,8}$	0.69 ± 0.19	0.53 ± 0.21
4	$M_{15,11}$	0.51 ± 0.21	0.35 ± 0.22
5	$M_{14,14}$	0.45 ± 0.18	0.59 ± 0.25
6	$M_{8,0}$	0.43 ± 0.24	0.54 ± 0.28
7	$M_{12,4}$	0.40 ± 0.24	0.52 ± 0.23
8	$M_{16,12}$	0.47 ± 0.18	0.38 ± 0.25
9	$M_{12,12}$	0.49 ± 0.21	0.60 ± 0.24
10	$M_{13,5}$	0.59 ± 0.22	0.67 ± 0.23

Table 6: List of most significant ($p<0.05$) Zernike moment features differentiating MCI and AD subjects using Radon transformed cerebellum images

S.No	Feature	MCI Subject	AD Subject
1	$M_{12,12}$	0.35 ± 0.21	0.60 ± 0.24
2	$M_{10,10}$	0.33 ± 0.22	0.58 ± 0.22
3	$M_{10,10}$	0.33 ± 0.22	0.58 ± 0.22
4	$M_{8,8}$	0.33 ± 0.22	0.58 ± 0.23
5	$M_{14,14}$	0.36 ± 0.2	0.59 ± 0.25
6	$M_{14,6}$	0.27 ± 0.17	0.44 ± 0.24
7	$M_{15,11}$	0.55 ± 0.22	0.35 ± 0.22
8	$M_{8,6}$	0.36 ± 0.21	0.57 ± 0.28
9	$M_{16,8}$	0.38 ± 0.19	0.54 ± 0.25
10	$M_{16,16}$	0.38 ± 0.19	0.52 ± 0.25

Table 7: List of most significant ($p<0.05$) Zernike moment features differentiating normal and MCI subjects using Hough transform cerebellum images

S.No	Feature	Normal Subject	MCI Subject
1	$M_{7,5}$	0.50 ± 0.18	0.65 ± 0.22
2	$M_{5,3}$	0.49 ± 0.18	0.64 ± 0.22
3	$M_{3,1}$	0.48 ± 0.18	0.63 ± 0.23
4	$M_{9,9}$	0.46 ± 0.21	0.61 ± 0.22
5	$M_{3,3}$	0.48 ± 0.18	0.61 ± 0.21
6	$M_{5,5}$	0.48 ± 0.18	0.62 ± 0.21
7	$M_{1,1}$	0.49 ± 0.18	0.63 ± 0.22
8	$M_{7,7}$	0.50 ± 0.19	0.64 ± 0.22
9	$M_{9,7}$	0.52 ± 0.19	0.65 ± 0.21
10	$M_{15,13}$	0.48 ± 0.20	0.36 ± 0.22

Table 8: List of most significant ($p<0.05$) Zernike moment features differentiating normal (0) and AD (1) subjects using Hough transform cerebellum images

S.No	Feature	Normal Subject	AD Subject
1	$M_{14,10}$	0.41 ± 0.21	0.59 ± 0.26
2	$M_{7,7}$	0.50 ± 0.19	0.37 ± 0.27
3	$M_{17,13}$	0.58 ± 0.23	0.44 ± 0.22
4	$M_{17,13}$	0.49 ± 0.19	0.40 ± 0.24
5	$M_{10,2}$	0.30 ± 0.21	0.42 ± 0.29
6	$M_{10,2}$	0.30 ± 0.21	0.42 ± 0.29
7	$M_{7,5}$	0.50 ± 0.18	0.41 ± 0.28
8	$M_{9,7}$	0.52 ± 0.19	0.44 ± 0.27
9	$M_{15,15}$	0.56 ± 0.23	0.46 ± 0.21
10	$M_{15,13}$	0.48 ± 0.2	0.57 ± 0.28

Table 9: List of most significant ($p<0.05$) Zernike moment features differentiating MCI (0.5) and AD (1) subjects using Hough transform cerebellum images

S.No	Feature	MCI Subject	AD Subject
1	$M_{7,7}$	0.64 ± 0.22	0.37 ± 0.27
2	$M_{7,5}$	0.65 ± 0.22	0.41 ± 0.28
3	$M_{14,10}$	0.37 ± 0.21	0.59 ± 0.26
4	$M_{5,5}$	0.62 ± 0.21	0.41 ± 0.26
5	$M_{9,9}$	0.61 ± 0.22	0.41 ± 0.25
6	$M_{5,3}$	0.64 ± 0.22	0.43 ± 0.26
7	$M_{9,7}$	0.65 ± 0.21	0.44 ± 0.27
8	$M_{3,1}$	0.63 ± 0.23	0.42 ± 0.25
9	$M_{15,13}$	0.36 ± 0.22	0.57 ± 0.28
10	$M_{5,1}$	0.63 ± 0.22	0.43 ± 0.26

differentiating the subjects with mild impairment.

The kurtosis and skewness accessed by the moments M4,0 and M5,1 show better discrimination between normal and MCI subjects. From Table 2 and 3 it can be observed that the higher order moments exhibit dominant abilities in differentiating AD from normal and MCI subjects with better significance. The features are found to have large overlap between the groups hence the features are analyzed from different space using Radon and Hough transform.

Table 4, 5 and 6 describe the statistical nature of Zernike moments obtained from Radon space of the cerebellum. It can be observed from the results the higher order moments show maximum differentiation between normal subjects and subjects with stages of AD. Literature conveys that the higher ordere moments recapitulate the nature of skewness and kurtosis based on the probability distribution of feature values over normal distribution. The features are observed to have high deviation between the subjects and groups which are reflected through the increased standard deviation. The higher order features are found to provide significant contribution towards to the classification of normal from MCI and AD subjects.

The significance of Zernike moments extracted from Hough space in differentiating normal from MCI and AD subjects are shown in Table 7, 8 and 9. It can be observed that the lower order moments obtained from Hough space show bet- ter discriminating ability in differentiating normal subjects from MCI subjects. The statistical nature of the features such as mean, varaiance, kurtosis and skewness are reflected in the lower order moments. The higher order moments are capable of differentiating AD subjects from MCI and control subjects.

Comparatively it can be observed that the moment features have the ability to differentiate the subjects groups. The higher order moments reflects the probability distribution na- ture of kurtosis and skewness effectively. The lower order moments are found be less significant is differentiating the disease catergories of AD.

V.Conclusions

Alzheimer's disease is found to have a preclinical phase which involves the alteration of cerebellum initiating the non-cognitive symptoms. In this analysis, structural alter- ation of cerebellum is analyzed for effective classification of disease categories. It is found that the orthogonal moment features are capable of identifying the minor alteration in the pixels which reflects the change in the boundary of cerebel- lum. Lower order moments are capable in differentiating nor- mal and AD subject but fails to differentiate MCI subjects from AD or control subjects effectively. Higher order mo- ments show promising ability in differentiating normal sub- jects from MCI and AD subjects with high significance.

Acknowledgments

The authors would like to thank Saveetha School of Engi- neering, Saveetha Institute of Medical and Technical Sci- ences (SIMATS) for their valuable support in completing the proposed work.

References

[1] A. J. Larner. The Cerebellum in Alzheimer's Disease, Dementia and Geriatric Cognitive Disorders, vol. 8, no. 4. pp. 203–209, 1997. doi: 10.1159/000106632.

[2] E. Hoxha et al. The Emerging Role of Altered Cere- bellar Synaptic Processing in Alzheimer's Disease, Frontiers in Aging Neuroscience, vol. 10. 2018. doi: 10.3389/fnagi.2018.00396.

[3] F. Bature, B.-A. Guinn, D. Pang, and Y. Pappas. Signs and symptoms preceding the diagnosis of Alzheimer's disease: a systematic scoping review of literature from 1937 to 2016, BMJ Open, vol. 7, no. 8. p. e015746, 2017. doi: 10.1136/bmjopen-2016-015746.

[4] C. Laske et al. Innovative diagnostic tools for early de- tection of Alzheimer's disease, Alzheimers. Dement., vol. 11, no. 5, pp. 561–578, May 2015.

[5] K. A. Johnson, N. C. Fox, R. A. Sperling, and W.

E. Klunk. Brain Imaging in Alzheimer Disease, Cold Spring Harb. Perspect. Med., vol. 2, no. 4, p. a006213, Apr. 2012.

[6] S. Huang,J. Li,J. Ye, T. Wu, K. Chen, A. Fleisher, and E. Reiman. Identifying Alzheimer's disease-related brain regions from multi-modality neuroimaging data using sparse composite linear discrimination analysis. Advances in neural information processing systems, 24, 2011.

[7] H. Yang et al. Study of brain morphology change in Alzheimer's disease and amnestic mild cognitive impairment compared with normal controls, General Psychiatry, vol. 32, no. 2. p. e100005, 2019. doi: 10.1136/gpsych-2018-100005.

[8] T. L. Jernigan et al. Effects of age on tissues and regions of the cerebrum and cerebellum, Neurobiol. Aging, vol. 22, no. 4, pp. 581–594, Jul. 2001.

[9] H. Fuse, K. Oishi, N. Maikusa, T. Fukami, Japanese Alzheimer's Disease Neuroimaging Initiative. Detec- tion of Alzheimer's disease with shape analysis of MRI images. In2018 Joint 10th International Conference on Soft Computing and Intelligent Systems (SCIS) and 19th International Symposium on Advanced Intelligent Systems (ISIS) 2018 Dec 5 (pp. 1031-1034). IEEE.

[10] E. Gerardin et al. Multidimensional classification of hippocampal shape features discriminates Alzheimer's disease and mild cognitive impairment from normal ag- ing, NeuroImage, vol. 47, no. 4. pp. 1476–1486, 2009. doi: 10.1016/j.neuroimage.2009.05.036.

[11] A. Sayeed, M. Petrou, N. Spyrou, A. Kadyrov, T. Spinks. Diagnostic features of Alzheimer's disease ex- tracted from PET sinograms. Physics in Medicine & Bi- ology. 2001 Dec 12;47(1):137.

[12] K. P. Philip, E. L. Dove, D. D. McPherson, N. L. Got- teiner, W. Stanford, and K. B. Chandran, The fuzzy Hough transform-feature extraction in medical images, IEEE Trans. Med. Imaging, vol. 13, no. 2, pp. 235–240, 1994.

[13] R. Pourreza-Shahri, M. Tavakoli, and N. Kehtarnavaz. Computationally efficient optic nerve head detection in retinal fundus images, Biomedical Signal Process- ing and Control, vol. 11. pp. 63–73, 2014. doi: 10.1016/j.bspc.2014.02.011.

[14] A. Burns, S. liffe. Alzheimer's disease. BMJ.;338:b158. 2009.

[15] B. Dubois, A. Padovani, P. Scheltens, A. Rossi, and G. Dell'Agnello. Timely Diagnosis for Alzheimer's Dis- ease: A Literature Review on Benefits and Challenges, J. Alzheimers. Dis., vol. 49, no. 3, pp. 617–631, 2016.

[16] B. C. Dickerson. Diagnostic tests for Alzheimer dis- ease: Judicious use can be helpful in clinical practice, Neurol. Clin. Pract., vol. 2, no. 2, pp. 154–157, Jun. 2012.

[17] X.-Q. Fu, L.-L. Zeng, F.-Q. Zhang, J.-L. Jiang, J.-T. Zhang, and H. Niu. Current status and future prospects of stem cell therapy in Alzheimer's disease, Neural Re- generation

Research, vol. 15, no. 2. p. 242, 2020. doi: 10.4103/1673-5374.265544.

[18] S. P. Cass. Alzheimer's Disease and Exercise: A Literature Review, Current Sports Medicine Re- ports, vol. 16, no. 1. pp. 19–22, 2017. doi: 10.1249/jsr.0000000000000332.

[19] G. M. McKhann et al. The diagnosis of dementia due to Alzheimer's disease: Recommendations from the National Institute on Aging-Alzheimer's Association workgroups on diagnostic guidelines for Alzheimer's disease, Alzheimer's & Dementia, vol. 7, no. 3. pp. 263–269, 2011. doi: 10.1016/j.jalz.2011.03.005.

[20] B. Dubois et al. Revising the definition of Alzheimer's disease: a new lexicon, Lancet Neurol., vol. 9, no. 11, pp. 1118–1127, Nov. 2010.

[21] E. G. Kehoe, J. P. McNulty, P. G. Mullins, and A. L. W. Bokde. Advances in MRI biomarkers for the diagnosis of Alzheimer's disease, Biomarkers in Medicine, vol. 8, no. 9. pp. 1151–1169, 2014. doi: 10.2217/bmm.14.42.

[22] G. Chetelat et al. Direct voxel-based comparison be- tween grey matter hypometabolism and atrophy in Alzheimer's disease, Brain, vol. 131, no. 1. pp. 60–71, 2007. doi: 10.1093/brain/awm288.

[23] S. Urooj, S. P. Singh, A. Malibari, F. Alrowais, and S. Kalathil. Early Detection of Alzheimer's Disease Us- ing Polar Harmonic Transforms and Optimized Wavelet Neural Network, Applied Sciences, vol. 11, no. 4. p. 1574, 2021. doi: 10.3390/app11041574.

[24] F. Ahmad and W. M. Dar. Classification of Alzheimer's Disease Stages: An Approach Using PCA-Based Algo- rithm, Am. J. Alzheimers. Dis. Other Demen., vol. 33, no. 7, pp. 433–439, Nov. 2018.

[25] N. Wang, F. Luo, V. Peddagangireddy, K. P. Subbalak- shmi, and R. Chandramouli. Personalized Early Stage Alzheimer's Disease Detection: A Case Study of Pres- ident Reagan's Speeches. Proceedings of the 19th SIG- BioMed Workshop on Biomedical Language Process- ing, arXiv preprint arXiv:2005.12385, 2020.

[26] A. B. Miled, T. Yeferny, and A.B. Rabeh. MRI Im- ages Analysis Method for Early Stage Alzheimer's Dis- ease Detection. IJCSNS International Journal of Com- puter Science and Network Security, arXiv preprint arXiv:2012.00830, 2020.

[27] F. Previtali, P. Bertolazzi, G. Felici, and E. Weitschek. A novel method and software for automatically clas- sifying Alzheimer's disease patients by magnetic reso- nance imaging analysis, Computer Methods and Pro- grams in Biomedicine, vol. 143. pp. 89–95, 2017. doi: 10.1016/j.cmpb.2017.03.006.

[28] U. R. Acharya et al. Automated Detection of Alzheimer's Disease Using Brain MRI Images– A Study with Various Feature Extraction Techniques, Journal of Medical Systems, vol. 43, no. 9. 2019. doi: 10.1007/s10916-019-1428-9.

[29] Y. Zhang, S. Wang, P. Phillips, J. Yang, and T.-
F. Yuan. Three-Dimensional Eigenbrain for the De- tection of Subjects and Brain Regions Related with Alzheimer's Disease, J. Alzheimers. Dis., vol. 50, no. 4, pp. 1163–1179, 2016.

[30] D. Jha, J. I. Kim, and G. R. Kwon. Diagnosis of Alzheimer's disease using dual-tree complex wavelet transform, PCA, and feed-forward neural network. Journal of healthcare engineering, 2017.

[31] X. Zhu and R. M. Rangayyan. Detection of the optic disc in images of the retina using the Hough transform, Conf. Proc. IEEE Eng. Med. Biol. Soc., vol. 2008, pp. 3546–3549, 2008.

[32] X. Zhu, R. M. Rangayyan, and A. L. Ells. Detection of the optic nerve head in fundus images of the retina us- ing the Hough transform for circles, J. Digit. Imaging, vol. 23, no. 3, pp. 332–341, Jun. 2010.
[33] M. Abdullah, M. M. Fraz, and S. A. Barman. Localiza- tion and segmentation of optic disc in retinal images us- ing circular Hough transform and grow-cut algorithm, PeerJ, vol. 4, p. e2003, May 2016.
[34] Z. Ma, B. Kang, K. Lv, and M. Zhao. Nonlinear radon transform using Zernike moment for shape analysis, Comput. Math. Methods Med., vol. 2013, p. 208402, Apr. 2013.
[35] D. S. Marcus, A. F. Fotenos, J. G. Csernansky, J. C. Morris, and R. L. Buckner. Open Access Series of Imaging Studies: Longitudinal MRI Data in Nonde- mented and Demented Older Adults, J. Cogn. Neu- rosci., vol. 22, no. 12, pp. 2677–2684, Dec. 2010.
[36] F. Faul, E. Erdfelder, A.-G. Lang, and A. Buch- ner, "G*Power 3: a flexible statistical power analy- sis program for the social, behavioral, and biomedi- cal sciences, Behav. Res. Methods, vol. 39, no. 2, pp. 175–191, May 2007.
[37] F. Faul, E. Erdfelder, A. Buchner, and A.-G. Lang. Sta- tistical power analyses using G*Power 3.1: Tests for correlation and regression analyses, Behavior Research Methods, vol. 41, no. 4. pp. 1149–1160, 2009. doi: 10.3758/brm.41.4.1149.

Author Biographies

Ramesh Munirathinam is currently working as Assistant Professor in the department of Biomedical Engineering, Karpagam Academy of Higher Education, Coimbatore, In- dia. Ramesh Munirathinam received his Bachelor Degree, Master Degree and Ph.D. from Anna University, Chennai, India. He received his Bachelor of Engineering in the depart- ment of Electronics and Communication Engineering. He did his Master of Engineering in the department of Control and Instrumentation. He carried out his research work in the field of Medical Image Processing. His research activ- ities involve early identification and diagnosis of rare dis- ease through non-invasive methodologies. He is an active researcher in the field of medical image and signal process- ing. He is also open to collaborative research activities.

Bhuvaneswari Balachander received her B.Tech Degree in Telecommunication Engineering from VIT University in the year 2008. She obtained her Masters in Communication Systems from Dr. M.G.R University in the year 2011. She received her Ph D in Medical Image Processing in the year 2020. Since 2012, she has been working as an Associate Professor in Saveetha School of Engineering, Chennai. She has around 11 years of teaching experience.